Interaction of the WD40 Domain of a Myoinositol Polyphosphate 5-Phosphatase with SnRK1 Links Inositol, Sugar, and Stress Signaling[1][W][OA]

Elitsa A. Ananieva, Glenda E. Gillaspy*, Amanda Ely, Ryan N. Burnette, and F. Les Erickson

Department of Biochemistry, Virginia Tech, Blacksburg, Virginia 24061 (E.A.A., G.E.G., R.N.B.); and
Department of Biology, Salisbury University, Salisbury, Maryland 21801 (A.E., F.L.E.)

In plants, myoinositol signaling pathways have been associated with several stress, developmental, and physiological processes, but the regulation of these pathways is largely unknown. In our efforts to better understand myoinositol signaling pathways in plants, we have found that the WD40 repeat region of a myoinositol polyphosphate 5-phosphatase (5PTase13; At1g05630) interacts with the sucrose nonfermenting-1-related kinase (SnRK1.1) in the yeast two-hybrid system and in vitro. Plant SnRK1 proteins (also known as AKIN10/11) have been described as central integrators of sugar, metabolic, stress, and developmental signals. Using mutants defective in 5PTase13, we show that 5PTase13 can act as a regulator of SnRK1 activity and that regulation differs with different nutrient availability. Specifically, we show that under low-nutrient or -sugar conditions, 5PTase13 acts as a positive regulator of SnRK1 activity. In contrast, under severe starvation conditions, 5PTase13 acts as a negative regulator of SnRK1 activity. To delineate the regulatory interaction that occurs between 5PTase13 and SnRK1.1, we used a cell-free degradation assay and found that 5PTase13 is required to reduce the amount of SnRK1.1 targeted for proteasomal destruction under low-nutrient conditions. This regulation most likely involves a 5PTase13-SnRK1.1 interaction within the nucleus, as a 5PTase13:green fluorescent protein was localized to the nucleus. We also show that a loss of function in 5PTase13 leads to nutrient level-dependent reduction of root growth, along with abscisic acid (ABA) and sugar insensitivity. *5ptase13* mutants accumulate less inositol 1,4,5-trisphosphate in response to sugar stress and have alterations in ABA-regulated gene expression, both of which are consistent with the known role of inositol 1,4,5-trisphosphate in ABA-mediated signaling. We propose that by forming a protein complex with SnRK1.1 protein, 5PTase13 plays a regulatory role linking inositol, sugar, and stress signaling.

Myoinositol (inositol) signaling pathways are important for many different developmental and physiological processes in eukaryotes (Boss et al., 2006; Berridge, 2007). In plants, inositol signaling is used in the response to abscisic acid (ABA; Sanchez and Chua, 2001; Xiong et al., 2001; Burnette et al., 2003; Gunesekera et al., 2007; Lee et al., 2007), salt stress (DeWald et al., 2001; Takahashi et al., 2001), gravity (Perera et al., 2001, 2006), and pathogens (Ortega and Perez, 2001; Andersson et al., 2006). The inositol signaling pathway makes use of an inositol 1,4,5-trisphosphate ($InsP_3$) second messenger that triggers intracellular Ca^{2+} release from various sources within the cell (Berridge, 1993; Tang et al., 2007), although the precise mechanism in plants is not yet known (Krinke et al., 2007). To terminate signaling events driven by $InsP_3$, cells utilize the myoinositol polyphosphate 5-phosphatases (5PTases; EC 3.1.3.56) to remove the 5-phosphate, thus initiating second messenger breakdown (Astle et al., 2007). Eukaryotes have a family of diverse 5PTases, with the Arabidopsis (*Arabidopsis thaliana*) genome containing 15 genes predicted to encode conserved 5PTases (Berdy et al., 2001). Of the 15 Arabidopsis 5PTase genes, four encode 5PTase enzymes with a large, N-terminal extension containing five to six WD40 repeat regions (Zhong and Ye, 2004). WD40 repeats are found in a number of eukaryotic regulatory proteins (Li and Roberts, 2001), where they are speculated to serve as a stable propeller-like platform to which proteins can bind either stably or reversibly. In some cases, sequences outside of the WD40 repeats may confer a new functional specificity to the protein even as conserved protein interactions are maintained through the WD40 repeats, potentially adapting basic cellular mechanisms to organism-specific processes. WD40-containing 5PTases are unique to plants and certain fungi, as no other genomes contain candidate genes for these proteins (Zhong and Ye, 2004).

By examining plants containing either a gain or loss of function in specific 5PTases, investigators have established that 5PTases are critical in plant develop-

ment and in ABA signaling. In particular, mutations in the *CVP2* (5PTase6; At1g05470) and 5PTase13 (At1g05630) genes have been linked to altered cotyledon vascular patterning and/or blue light responses and phototropin 1 signaling (Carland and Nelson, 2004; Lin et al., 2005; Chen et al., 2008). In contrast, *fra3* (At1g65580) and *mrh3* (5PTase5; At5g65090) mutants are altered in fiber cell development (Zhong et al., 2004) and root hair initiation (Jones et al., 2006), respectively. With regard to stress signaling, ectopic expression of either 5PTase1 or 5PTase2 has been shown to decrease ABA signaling by increasing hydrolysis of $InsP_3$ (Sanchez and Chua, 2001; Burnette et al., 2003). Loss-of-function mutants in these same genes result in ABA hypersensitivity in germinating seeds and increased seedling hypocotyl elongation in the dark, which is accompanied by an increase in $InsP_3$ levels (Gunesekera et al., 2007).

5PTases have been reported to play a role in Glc sensing/metabolism in animal cells (Wada et al., 2001; Sasaoka et al., 2004; Kagawa et al., 2008). Overexpression of an SH2-containing inositol phosphatase 2 (SHIP2) inhibited insulin-induced signaling leading to Glc uptake and glycogen synthesis via hydrolysis of phosphatidylinositol 3,4,5-trisphosphate ($PtdIns-P_3$) in 3T3-L1 adipocytes and L6 myotubes (Sasaoka et al., 2001; Wada et al., 2001). On the other hand, loss of SHIP2 in mice resulted in increased sensitivity to insulin, which is characterized by deregulated expression of genes involved in gluconeogenesis and perinatal death (Clement et al., 2001). Although there are recent reports delineating some relationship between inositol signaling and sugar sensing/metabolism in plant cells (Im et al., 2007; Lou et al., 2007), a specific role of 5PTases in sugar signaling has not yet been determined. The mechanisms by which plants sense sugars and regulate carbohydrate metabolism are complex and often facilitated by protein complexes. Therefore, we sought to identify 5PTase-interacting proteins involved in signaling and metabolic events.

We report here that the WD40 repeat region of the 5PTase13 gene interacts specifically with a Suc nonfermenting-1-related kinase (SnRK1.1, AKIN10; At3g01090), which functions as a sensor of energy and stress in plants (Baena-Gonzalez et al., 2007; Hardie, 2007; Hue and Rider, 2007). Using T-DNA insertion mutants in the 5PTase13 gene, we present evidence that 5PTase13 is a nuclear protein that can act as a regulator of SnRK1.1 under low-nutrient conditions by decreasing the amount of SnRK1.1 degraded by the proteasome.

RESULTS

5PTase13 Is a Member of a Unique Group of WD40-Containing Proteins

Besides containing a conserved inositol polyphosphate 5-phosphatase catalytic domain, 5PTase13 also contains five WD40 repeat regions in the N terminus that may allow for unique protein interactions. Three other genes in the Arabidopsis genome, 5PTase12 (At2g43900), 5PTase14 (At2g31830), and FRA3 (At1g65580), encode similar proteins (Berdy et al., 2001; Zhong and Ye, 2004), and the amino acid identity of the WD40 repeat region varies from 45.5% to 75.3% among these proteins (Supplemental Table S1). We used the amino acid sequences corresponding to these WD40 repeat regions in BLASTp searches and obtained 12 related sequences with e-values less than 1. ClustalW and PAUP4.0 were used to generate phylogenetic trees using parsimony (Fig. 1), which showed that the 5PTase WD40 repeat regions are contained on a separate branch, thus indicating that they are more similar to one another than to other WD40 repeat regions.

The similarity of the 5PTases (Zhong and Ye, 2004) suggests that these proteins may function in a redundant manner. Microarray data from GENEVESTIGATOR (Zimmermann et al., 2004) indicates that FRA3 is broadly and abundantly expressed compared with 5PTase12, 5PTase13, and 5PTase14 (Supplemental Fig. S1A). We conclude that the WD40-containing 5PTases are a small group of proteins with the potential to form protein complexes and that functional redundancy may be present.

The WD40 Repeat Region of 5PTase13 Interacts with SnRK1.1

To investigate the ability of the WD40 regions of 5PTase13 to participate in protein complexes, we used the yeast two-hybrid system. The 533 N-terminal amino acids from 5PTase13 containing the WD40 repeats were used as bait in a yeast two-hybrid screen of an Arabidopsis 3-d-old etiolated seedling cDNA library. We screened over 1 million yeast transformants and obtained a positive clone containing the C-terminal domain of the SnRK1.1 gene (At3g01090; also known as AKIN10). We retransformed this positive clone into yeast and verified the interaction (Fig. 2). Negative controls, including the empty DNA binding domain and activation domain vectors, established that SnRK1.1 binds to the WD40 repeat region of the 5PTase13 protein in yeast.

To examine the interaction between 5PTase13 and SnRK1.1 in vitro, we fused the sequence encoding the Xpress epitope tag to the C terminus of the WD40 repeat region of 5PTase13 (13WDX) and the V5 epitope tag sequence to the C terminus of SnRK1.1 (SnRKV5) and expressed both proteins in *Escherichia coli*. The SnRKV5 construct directs the expression of a 61.7-kD protein detected by an anti-V5 monoclonal antibody, and in most cases we detected two SnRKV5 bands, perhaps as a result of phosphorylation or proteolytic cleavage (Fig. 3, lane 1). The 13WDX construct directs the expression of a 65.9-kD protein detected by an anti-Xpress monoclonal antibody (Fig. 3, lane 2). These interactions are specific, as SnRKV5 is not detected by

Figure 1. Phylogenetic tree of the WD40 regions from 5PTases and other WD40-containing Arabidopsis proteins. ClustalW and PAUP4.0 were used to generate a tree. Bootstrapping (1,000 times) yielded the confidence level indicated at each branch. The results show that the WD40 region of 5PTase14 (14WD) is the closest relative to 5PTase13 (13WD). Furthermore, the tree indicates that the 5PTase WD40 regions (12WD, 13WD, 14WD, and FRA3WD) are more closely related to each other than to other WD40-containing proteins.
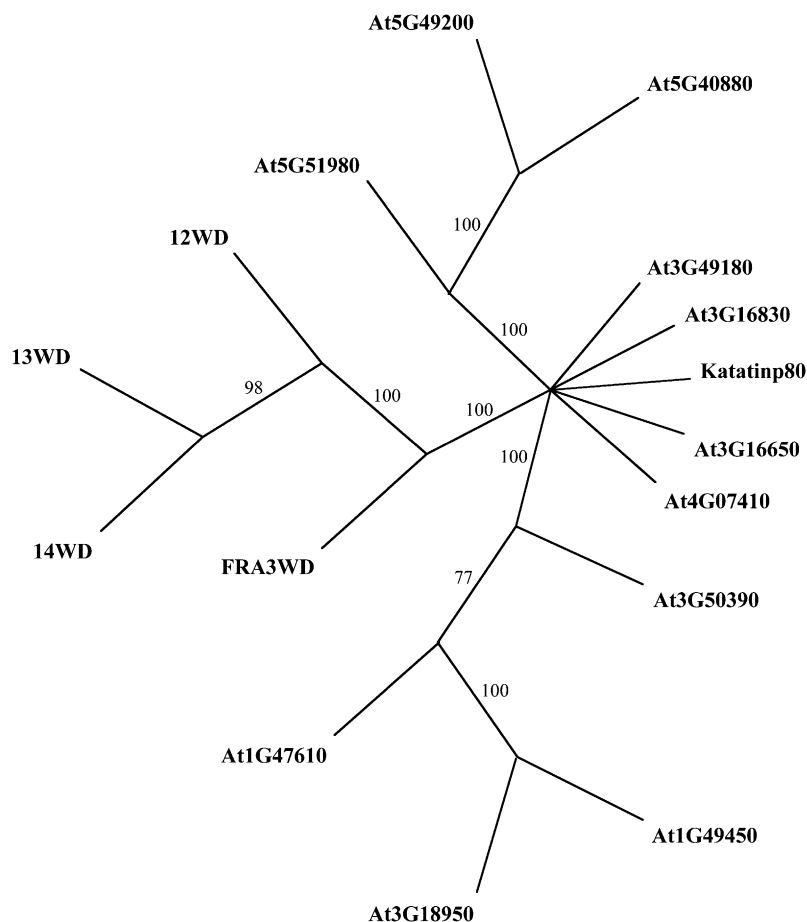
the anti-Xpress antibody and 13WDX is not detected by the anti-V5 antibody (data not shown). To determine whether the SnRK1.1 recombinant protein can "pull down" 13WDX, immunoprecipitations using anti-V5:protein A-Sepharose beads were performed, and the resulting complex was then analyzed by western blotting with an anti-Xpress antibody (Fig. 3, IP lanes). As shown in Figure 3, the WD40 repeat region from 5PTase13 (13WDX) is only detected in this pull-down assay when it has been incubated in the presence of SnRKV5. We conclude that the WD40 repeat region from 5PTase13 and SnRK1.1 can form a protein complex in vitro.

SnRK1.1, along with its closely related gene family member SnRK1.2, encodes a Suc nonfermenting-1-related kinase implicated as a central integrator of energy signaling and metabolic regulation in yeast, plants, and animals. The interaction of 5PTase13 and SnRK1.1 is novel and is perhaps unique to plants in that yeast and animal 5PTases do not contain WD40 regions. This interaction may indicate that InsP$_3$ signal termination via 5PTase13 function affects the SnRK1 "energy sensor" in plants. Data obtained from the GENEVESTIGATOR database indicate that SnRK1.1, SnRK1.2, and 5PTase13 are detected in most plant tissues examined, although 5PTase13 expression levels are very low compared with SnRK1 gene expression (Supplemental Fig. S1B).

5PTase13 Mutant Identification

To further explore the link between InsP$_3$ signaling and the energy sensor, SnRK1.1, we isolated two independent T-DNA insertion mutants in the 5PTase13 gene. Two potential mutants were identified in the SALK T-DNA database and named *5ptase13-1* (SAIL_350_FO1) and *5ptase13-2* (SALK_081991) and were compared with their corresponding wild-type accessions (Fig. 4A). The presence of the T-DNA insertion was verified by diagnostic PCR in each mutant using genomic DNA and primers specific for the T-DNA left border (LB) and gene-specific primers that flank the T-DNA insertion (Fig. 4, A and B). The resulting LB gene-specific fragments were sequenced, indicating that in *5ptase13-1* mutants, a second T-DNA insertion is found in tandem in the fourth exon (Fig. 4, A and B, LB-R band). This is in contrast to the previously reported analysis by Lin et al. (2005) showing that the *5ptase13-1* mutant contains a single T-DNA insertion.

Using primers specific for the 3' end of 5PTase13, we detected a PCR product in both wild-type lines used
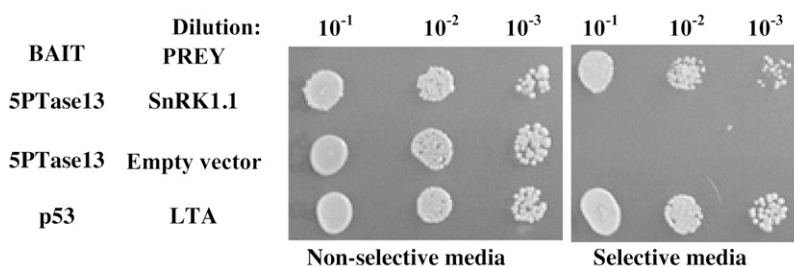
Figure 2. Yeast two-hybrid screen. An Arabidopsis cDNA prey library was screened using the WD40 region of 5PTase13 as a bait in the yeast two-hybrid system. Over 1 million yeast transformants were screened for reporter gene expression, which resulted in the isolation of a prey plasmid expressing the C-terminal domain of SnRK1.1. Serially diluted yeast strains were spotted onto agar plates that are either nonselective or selective for expression of the two-hybrid reporter genes.

(CS60000 and CS908) but not in *5ptase13-1* and *5ptase13-2* mutants (5PTase13 in Fig. 4C). Using primers that amplify the 5′ end, we detected a 1.68-kb product in both wild-type lines and in the *5ptase13-1* mutant, but not in *5ptase13-2* (Fig. 4C). We conclude that the *5ptase13-2* mutant is totally lacking 5PTase13 expression and that both *5ptase13-1* and *5ptase13-2* mutant lines do not express transcripts capable of encoding a full-length 5PTase13 protein.

To examine how the loss of 5PTase13 affects the expression of its binding partner SnRK1.1, we examined the expression of SnRK1.1 and its closely related isoform, SnRK1.2, in 7-d-old dark-grown *5ptase13* and wild-type seedlings. The results reveal that there are no large changes in SnRK1.1 and SnRK1.2 in *5ptase13* mutants (Fig. 4D). As shown in Figure 4D, we found that FRA3 expression remains unchanged in *5ptase13* mutants, and 5PTase14 expression is barely detectable but also unchanged. In contrast, the expression of 5PTase12 is increased in both *5ptase13* mutant lines, revealing a possible means of compensation for the loss of 5PTase13 function (Fig. 4D).

Under standard laboratory conditions, *5ptase13* mutants did not exhibit any abnormalities in plant growth or development. Since Lin et al. (2005) previously reported that *5ptase13-1* mutants are altered in cotyledon vein development, we carefully examined both *5ptase13-1* and *5ptase13-2* mutants and their corresponding wild-type accessions for cotyledon vein development, as described by Carland and Nelson (2004). Using 7-d-old light-grown seedlings of wild-type and *5ptase13* mutant soil-grown plants, we found no evidence for a cotyledon vein phenotype (Supplemental Tables S2 and S3). Our analysis revealed that 33.3% of total WT1 cotyledons and 26.18% of total *5ptase13-1* cotyledons have abnormal patterns and that only 15.9% of total WT2 cotyledons and 19.4% of total *5ptase13-2* cotyledons can be classified as abnormal (Supplemental Table S3). Thus, there is variation in cotyledon vein development within different wild-type accessions, but not between *5ptase13* mutants and their matched wild-type accessions.

SnRK1 Activity Is Altered in *5ptase13* Mutants and Varies with Nutrient Conditions

To determine whether 5PTase13 affects SnRK1 function, we measured the activity of SnRK1 in *5ptase13* mutants and wild-type seedlings grown under various nutrient conditions. It is well documented that SnRK1 regulates multiple transcription cascades in response to sugar or energy deprivation (Baena-Gonzalez et al., 2007); however, whether in planta SnRK1 activity changes under various nutrient conditions is not known. To address this, we measured SnRK1 activity from 7-d-old wild-type seedlings grown under low light (40 μE) with different added nutrients to establish various "low-energy" conditions: no nutrients (agar and water alone), low nutrients (0.5× Murashige and Skoog [MS] salts and agar), and optimal nutrients (0.5× MS salts, agar, and 3% Suc). In addition, we examined a stressful level of added sugar (0.5× MS salts, agar, and 6% Glc). For this work, we used a well-

Figure 3. 13WD40-Xpress protein interacts with SnRK1.1-V5 in vitro. Immunoprecipitation (IP) was carried out using an anti-V5 antibody bound to a protein A-Sepharose (PAS). Purified and dialyzed proteins (13WDX and SnRKV5) were incubated for 2 h at room temperature in immunoprecipitation buffer before transferring to the antiV5:PAS complex. The resulting immunoprecipitation fractions were analyzed using protein gel blotting. Lane 1, Input fraction of SnRKV5 probed with an anti-V5 antibody; lane 2, input fraction of 13WDX; lane 3, input fraction of 13WDX in combination with SnRKV5; lane 4, bound fraction of 13WDX alone; lane 5, bound fraction of 13WDX in combination with SnRKV5. Lanes 2 through 5 were probed with an anti-Xpress antibody. The 55-kD band is the immunoglobin heavy chain component of the anti-V5 antibody. The blot images are representative of four independent experiments.
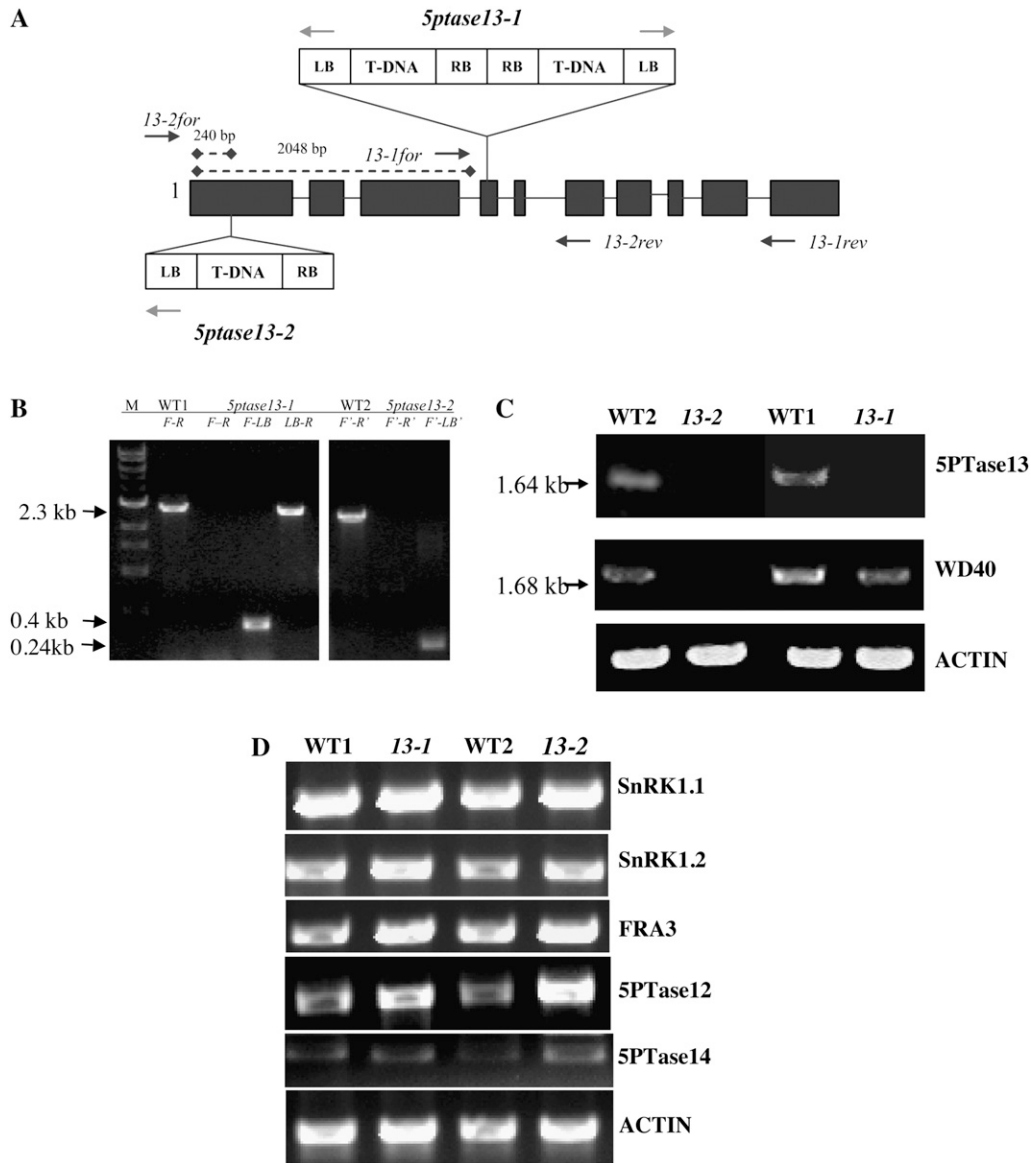
Figure 4. T-DNA insertions and gene expression in *5ptase13* mutant lines. A, T-DNA insertions in the 5PTase13 gene. Exons are shown as dark gray boxes; light gray arrows indicate primers used to amplify the LB of the T-DNA; dark gray arrows indicate positions of gene-specific primers. RB, Right border. B, PCR performed with gene-specific and LB primers confirms that both lines are homozygous. Gene-specific primers that flank the T-DNA insertion (primers *13-1for* [F] and *13-1rev* [R]) in conjunction with the T-DNA LB primer amplify 0.4- and 2.3-kb fragments in *5ptase13-1* mutants, indicating the presence of two LB sequences in proximity to the 5PTase13 gene. C and D, Expression of genes in *5ptase13* and wild-type seedlings. Total RNA (1–2 µg) was isolated, and semiquantitative RT-PCR was performed with the indicated primers (Supplemental Table S4). C, Verification of the loss of 5PTase13 expression in 2-week-old leaves from soil-grown plants. D, SnRK1 and 5PTase expression from 7-d-old wild-type and *5ptase13* (*13-1* and *13-2*) seedlings grown on 0.5× MS salts and 0.8% agar in the dark. The experiment was independently repeated two times.

established SnRK1 assay (Radchuk et al., 2006) and incubated a sucrose phosphate synthase (SPS) substrate peptide (Huang and Huber, 2001), radiolabeled [γ-^{32}P]ATP, and 5 µg of plant protein extract for 30 min. Validation that these conditions are in the linear range of product accumulation is shown in Supplemental Figure S2.

As expected from its role as a low-energy sensor, SnRK1 activity is higher in seedlings grown on low nutrients compared with extracts prepared from seedlings grown on optimal nutrients or 6% Glc (Fig. 5). Figure 6A shows that the activity of SnRK1 significantly increases in *5ptase13-1* and *5ptase13-2* mutants when seedlings are grown with no nutrients (8.1- and
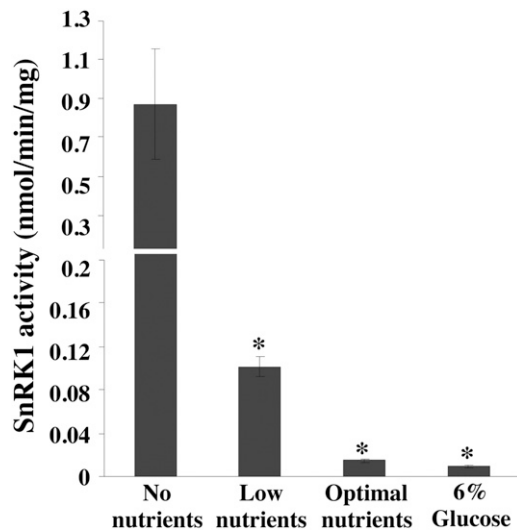
Figure 5. SnRK1 activity varies with different nutrient conditions. Seeds from wild-type (WT2-CS60000) plants were grown on 0.8% agar, no nutrients, low nutrients (0.5× MS salts), optimal nutrients (0.5× MS salts, 3% Suc), or 6% Glc (0.5× MS salts, 6% Glc) under low light for 7 d. The seeds grown in 6% Glc were allowed to germinate in 0.5× MS medium for 4 d and then transferred to 6% Glc medium for 3 d. SnRK1 activity with an SPS peptide was measured from crude plant extracts precipitated with ammonium sulfate according to the method described (Radchuk et al., 2006). Bars represent means ± SE of three replicates. The experiment was independently repeated two times. *, $P < 0.05$ compared with no nutrients.

11.3-fold increases, respectively). In contrast, SnRK1 activity decreases in *5ptase13-1* and *5ptase13-2* seedlings compared with wild-type seedlings when grown with low nutrients (Fig. 6B). Furthermore, the decline in SnRK1 activity is even more dramatic when 6% Glc is added (7.1- and 3.3-fold reduction, respectively; Fig. 6C). We conclude that a loss of 5PTase13 function affects SnRK1 activity, and the impact differs depending on nutrient availability. Our data support a role for 5PTase13 as a negative regulator of SnRK1 activity in the absence of nutrients and as a positive regulator when either low nutrients or 6% Glc is present.

5PTase13 Affects SnRK1.1 Stability

To explore whether 5PTase13 regulates SnRK1.1 stability, we used a similar approach as Lee et al. (2008) to examine the stability of recombinant V5-tagged SnRK1.1 (SnRKV5) in a cell-free degradation assay with wild-type or *5ptase13* extracts. The time course of SnRKV5 degradation with wild-type seedling extracts indicated that SnRKV5 is mostly degraded within 60 min (Fig. 7A). MG132, a proteasome-specific inhibitor, blocked SnRKV5 degradation in both *5ptase13* and wild-type extracts (Fig. 7B), indicating that SnRKV5 is destroyed by the 26S proteasome pathway in these assays.

To test the hypothesis that 5PTase13 destabilizes SnRK1.1 under the no-nutrient conditions, we examined a 30-min time point for analysis as a midpoint to total SnRKV5 degradation. The data indicate no difference in SnRKV5 stability in wild-type and *5ptase13* extracts under the no-nutrient conditions (Fig. 7C). In contrast, when extracts are prepared from seedlings grown on low nutrients, we find less SnRKV5 accumulation in *5ptase13* extracts compared with wild-type extracts (Fig. 7D). We conclude that under the low-nutrient conditions, 5PTase13 is required to stabilize SnRKV5 protein and slow its degradation by the 26S proteasome pathway. Furthermore, the increased degradation of SnRKV5 seen with the low-nutrient conditions correlates well with the lower SnRK1 activity levels measured in *5ptase13* mutants under these same nutrient conditions (Fig. 6B). In contrast, 5PTase13 is not required to stabilize SnRKV5 when seedlings are grown with no nutrients, and this is consistent with the switch in SnRK1 activity levels we found in *5ptase13* mutants grown with no nutrients (Fig. 6A). However, since we did not observe an increase in SnRKV5 stability in *5ptase13* extracts prepared from the no-nutrient conditions, we speculate that there is an additional mechanism that influences the elevated SnRK1 activity in *5ptase13* mutants under these conditions.

Role of 5PTase13 in Root Growth under Different Nutrient Conditions

We compared *5ptase13* mutants with SnRK1.1 mutants, which have a small reduction in root growth under the low-nutrient conditions and exhibit enhanced root growth with 1% to 3% Suc (Baena-Gonzalez et al., 2007). *5ptase13-1* and *5ptase13-2* mutants exhibited reduced root growth under no-nutrient and low-nutrient conditions and no change in root growth when exogenously supplied with 3% Suc (Fig. 8, A–C). A similar trend in nutrient-dependent root growth reduction of *5ptase13* mutants was also found when seedlings were grown in the dark (data not shown). This indicates that along with a decrease in SnRK1 activity (Fig. 6B), *5ptase13* mutants grown on the low-nutrient conditions have the same root phenotype as the SnRK1.1 mutants (Baena-Gonzalez et al., 2007), suggesting that the decrease in root growth may be an outcome of decreased SnRK1 activity. However, since the *5ptase13* mutants grown with no nutrients have elevated SnRK1 activity (Fig. 6A), we conclude that under these conditions the decrease in *5ptase13* mutant root growth cannot be a function of lower SnRK1 activity and most likely involves another mechanism.

5PTase13 Alterations Change Plant Sensitivity to Sugars and ABA

To test whether 5PTase13 is required for sugar and ABA responses, we analyzed age-matched seeds for germination in the presence of 0%, 1%, 3%, or 6% Glc
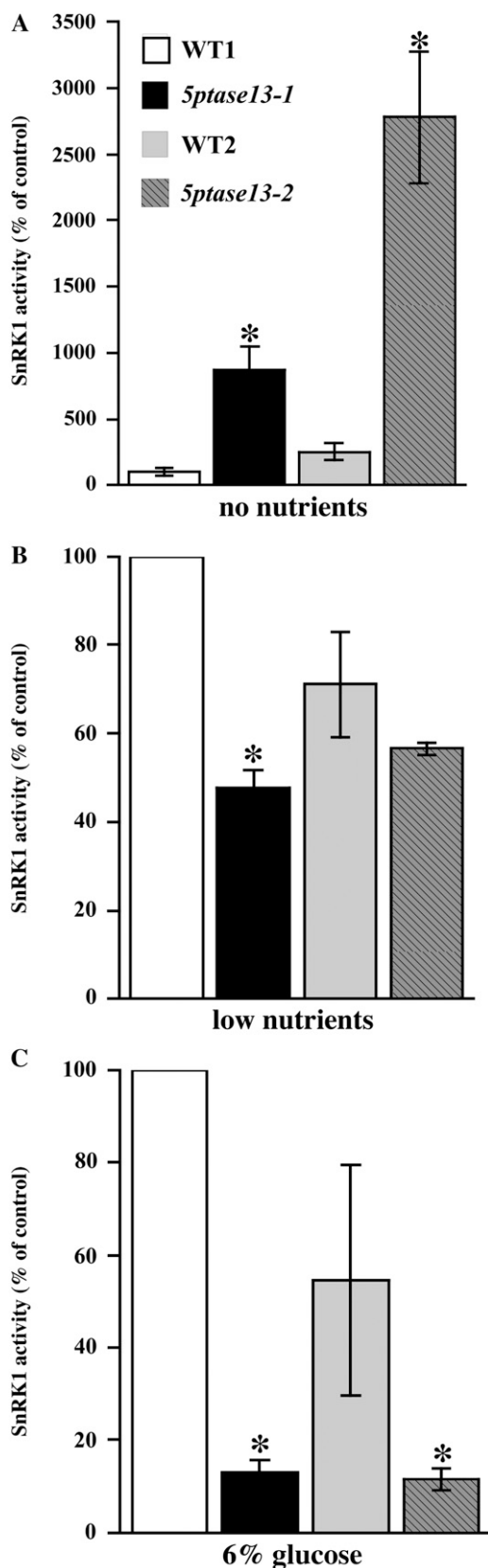
Figure 6. SnRK1 activity in *5ptase13* mutants. SnRK1 activity was measured in crude plant extracts from 7-d-old seedlings precipitated with ammonium sulfate according to the method described (Radchuk et al., 2006) using an SPS peptide. Values for SnRK1 activity (nmol inorganic phosphate min^{-1} mg^{-1} protein) are normalized to WT1. Extracts are from seedlings grown in no nutrients (A), low nutrients (0.5× MS salts; B), or 6% Glc (0.5× MS salts, 6% Glc; C). Bars represent means ± SE of three replicates. The experiment was independently repeated two times. *, $P < 0.05$ compared with the wild type.

or 0%, 1%, 2%, 3%, 6%, or 11% Suc. At low concentrations of sugar, there were no differences in the germination of wild-type and *5ptase13* seeds in the dark or light (data not shown). However, at a high exogenous sugar concentration (6% Glc and 11% Suc) in the dark, we found that *5ptase13* mutants were significantly less sensitive to sugar (Fig. 8D; Supplemental Figs. S3 and S4). We saw the same trend in sugar insensitivity when *5ptase13* mutant seeds were germinated in the presence of 6% Glc in the light, although the sugar insensitivity was less apparent (Supplemental Fig. S3). This sugar insensitivity was also noted for *5ptase13-1* and *5ptase13-2* mutant seeds germinated in the presence of 11% Suc, in which maximal increases of 2.5- and 2.2-fold for *5ptase13-1* and *5ptase13-2*, respectively, were noted compared with wild-type seeds (Supplemental Fig. S4). Germination in the presence of mannitol, a nonmetabolizable sugar, was not altered, indicating that the sugar insensitivity of *5ptase13* mutants is not due to a general osmotic stress tolerance (Fig. 8D).

We also germinated *5ptase13* mutant seeds in the presence of 0, 1, 2, and 3 μM ABA and measured the impact on germination during a 6-d period. As expected, germination of wild-type seeds was delayed by ABA in a concentration-dependent manner during the 6-d period under light conditions (Fig. 8, E and F). In contrast, *5ptase13-1* and *5ptase13-2* mutant seeds were ABA insensitive, reaching 100% germination on day 2 in the presence of 1 μM ABA and 78% to 90% on day 6 in the presence of 3 μM ABA (Fig. 8, E and F). Since we did not find reduced seed dormancy in our mutants (data not shown), this ABA insensitivity of *5ptase13* mutants most likely does not correlate with changes in de novo synthesis of ABA (Gubler et al., 2005) and is in accordance with the previously reported results for ABA insensitivity of the *5ptase13-1* mutant (Lin et al., 2005).

Expression of Glc- and ABA-Regulated Genes Is Altered in *5ptase13* Mutants

To determine whether there are differences in the expression patterns of Glc- and/or ABA-regulated genes (*RD29A*, *KIN1*, and *CAB1* genes; Price et al., 2004) in *5ptase13* mutants, we examined expression in 4-d-old dark-grown wild-type and *5ptase13* seedlings exposed to 6% Glc for 3 d (Fig. 9A). Treatment with 6% Glc strongly induced the expression of *RD29A* and *KIN1* in wild-type seedlings. In contrast, *5ptase13-1*
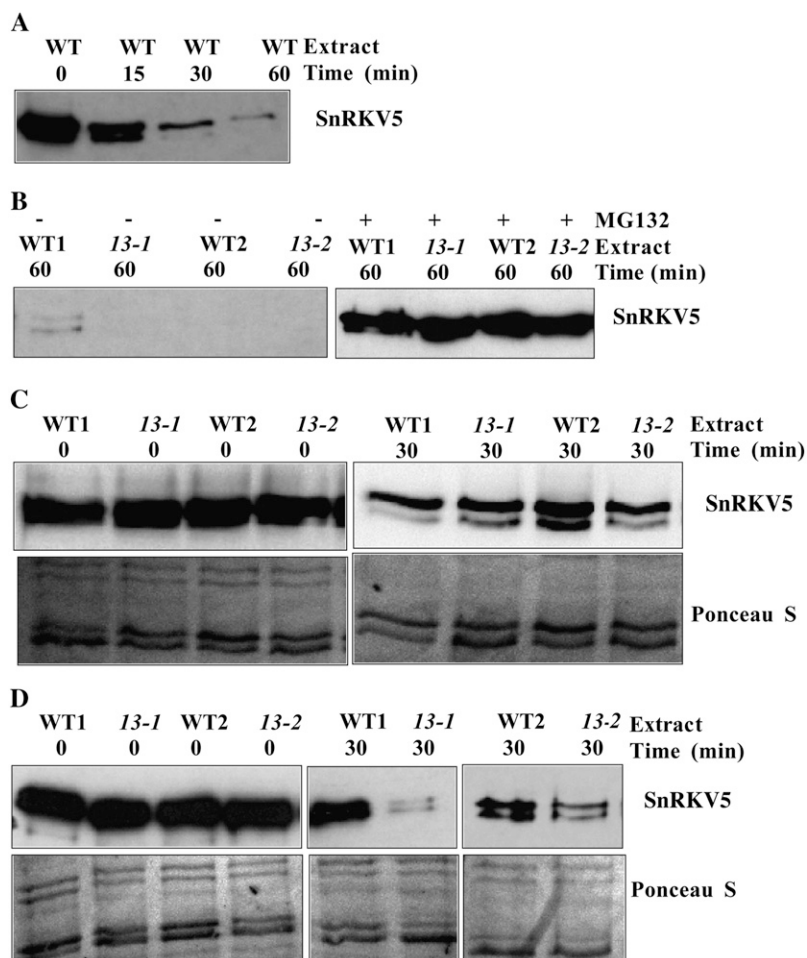
Figure 7. Degradation of V5-tagged SnRK1.1 in cell extracts from wild-type (WT) and *5ptase13* seedlings grown under different nutrient conditions. SnRK1.1-V5 protein (SnRKV5; 500 ng) was incubated in extracts (30 μg) prepared from 7-d-old light-grown wild-type and *5ptase13* seedlings for the indicated times at 30°C and was analyzed by western blotting with an anti-V5 antibody. A and B, Extracts from seedlings grown on low nutrients were incubated in the presence or absence of 10 μM MG132. C, SnRKV5 protein degradation in extracts prepared from seedlings grown with no nutrients. D, SnRKV5 protein degradation in extracts prepared from seedlings grown with low nutrients (0.5× MS salts). Ponceau S-stained filters are shown as controls for equivalent loading. The blot images are representative of two independent experiments.

and *5ptase13-2* mutants grown in 6% Glc contained much smaller increases in *RD29A* and *KIN1* transcript levels (Fig. 9A), indicating that induction of these genes is diminished, but not abolished, in *5ptase13* mutants. The regulation of CAB1, on the other hand, was not significantly altered in *5ptase13* mutants.

Complementation of the *5ptase13-1* Mutant

To ensure that the alterations noted in *5ptase13* mutants are due to loss of 5PTase13 expression, we expressed a 5PTase13:GFP fusion under the control of the 35S cauliflower mosaic virus promoter in wild-type and *5ptase13-1* plants (13:GFP and *13-1*/13:GFP plants, respectively). We examined two lines of *13-1*/13:GFP plants with good expression of the transgene (Fig. 9B) along with wild-type and *5ptase13-1* plants in ABA-sensitivity assays. Both *13-1*/13:GFP lines exhibited more ABA sensitivity in germination assays compared with *5ptase13* mutants (Fig. 9C). Since *5ptase13-1* mutants contain decreased SnRK1 activity under low-nutrient conditions compared with wild-type plants (47%; Fig. 6B), we also measured SnRK1 activity in the *13-1*/13:GFP-1 and *13-1*/13:GFP-2

lines and found, as expected, similar or increased SnRK1 activity compared with wild-type plants (140% ± 10% for *13-1*/13:GFP-1 and 102% ± 5% for *13-1*/13:GFP-2). We conclude that expression of the 5PTase13:GFP transgene complements the *5ptase13-1* mutant.

Glc-Stimulated InsP$_3$ Levels Are Altered in *5ptase13* Mutant Seedlings

We examined whether the Glc insensitivity of *5ptase13* mutants is accompanied by alterations in mass InsP$_3$ levels by measuring mass InsP$_3$ levels. The results in Figure 10 indicate that neither *5ptase13-1* nor *5ptase13-2* mutant seedlings differ significantly from wild-type seedlings in their InsP$_3$ mass levels under control conditions. When wild-type seedlings are exposed to 6% Glc for 3 d, mass InsP$_3$ levels increase 2.8- to 3.7-fold, which is a statistically significant elevation. However, when *5ptase13* mutants are grown for 3 d in the presence of 6% Glc, mass InsP$_3$ level changes are smaller, with an increase of 1.6- to 2-fold over basal levels, and statistically significant only in the *5ptase13-2* mutant. More importantly, the
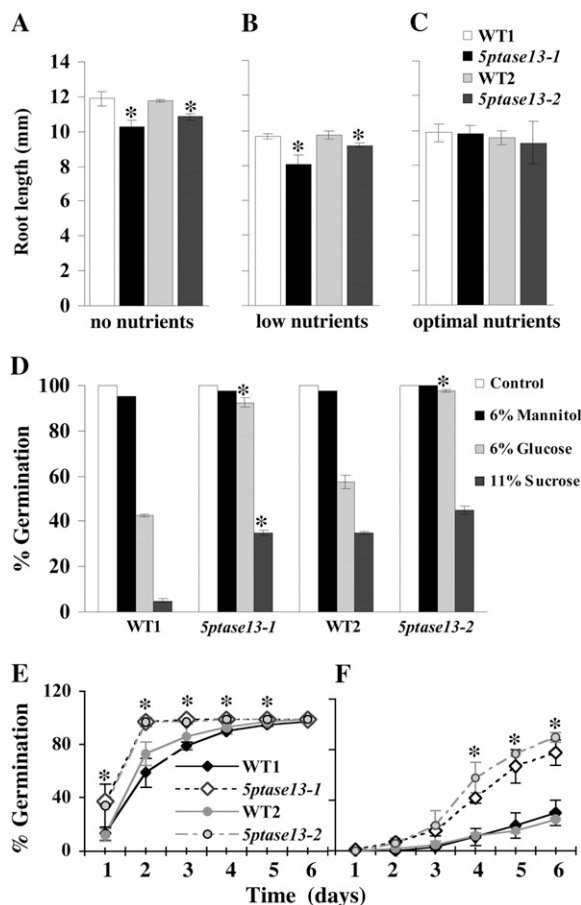
Figure 8. Phenotypes of *5ptase13* mutants. A to C, Roles of 5PTase13 in root development under different nutrient conditions. Wild-type and *5ptase13* mutant (*13-1* and *13-2*) seeds were grown in low light for 6 d on 0.8% agar plates and no nutrients (A), low nutrients (0.5× MS salts; B), or optimal nutrients (0.5× MS salts, 3% Suc; C). The root length for each group of seedlings was measured on days 2, 4, and 6. The results represent the root length measured after 4 d. Values are means ± SE ($n \geq$ 40). The experiment was independently repeated two times. D, Comparison of germination of wild-type and *5ptase13* seeds grown on 0.5× MS salts and 0.8% agar that were untreated (control) or treated with 6% Glc, 6% mannitol, or 11% Suc after 7 d in the dark. Values are means ± SE (n = 50). The data are representative of three independent experiments. E and F, Wild-type and *5ptase13* mutant seeds were germinated in the light for 6 d on 0.5× MS salts, 0.8% agar, and either 1 μM ABA (E) or 3 μM ABA (F). The germination rate was scored for each group of seeds starting from day 1. Values are means ± SE (n = 50). Significant differences from wild-type germination were noted at days 1 to 5 for *5ptase13-1* (1 μM ABA) and days 4 to 6 for both mutants (3 μM ABA). The experiment was independently repeated two times. *, $P < 0.05$ compared with the wild type.

Glc-stimulated InsP$_3$ levels in both *5ptase13* mutants differ significantly from the Glc-stimulated InsP$_3$ levels in wild-type seedlings. We conclude that *5ptase13* mutants are impaired in their ability to accumulate InsP$_3$ in response to Glc and that this correlates with the sugar and ABA insensitivity noted in the germination assays.

Subcellular Localization of the 5PTase13:GFP Fusion Protein

To investigate the subcellular location of the 5PTase13 protein, we performed imaging experiments with *5ptase13-1* mutants complemented with the 5PTase13:GFP construct (*13-1*/13:GFP plants) and wild-type plants containing the same 5PTase13:GFP construct. As the 5PTase13:GFP construct we used allowed for complementation of the ABA and sugar insensitivity phenotype in *5ptase13-1* mutants (Fig. 9, B and C), it is likely that this fusion protein undergoes the same posttranslational modifications and subcellular localization as the native 5PTase13 protein. We analyzed T2 progeny from two independent *13-1*/13: GFP lines with fluorescence deconvolution microscopy and found a similar pattern in both lines. GFP fluorescence was associated with the nucleus in many, but not all, cells in cotyledon epidermis (Fig. 11, B and C), hypocotyls (data not shown), and roots (Fig. 11, D–I). Nuclei from some but not all guard cells contained the 13:GFP protein (Fig. 11C). To confirm the nuclear localization, we stained *13-1*/13:GFP seedlings with the nuclear dye 4',6-diamidino-2-phenylindole (DAPI) and imaged GFP and DAPI fluorescence simultaneously (Fig. 11, D–I). Once again, we found 13:GFP fluorescence in only a portion of root nuclei, while DAPI fluorescence was present in all nuclei. We conclude that 5PTase13 protein is located in the nucleus of seedlings and that its presence in the nucleus is restricted in some cells.

DISCUSSION

Since control of second messengers is critical for signaling, there is interest in determining how the plant cell regulates levels of second messengers such as InsP$_3$. We identified a potential regulator of InsP$_3$ signaling by isolating protein interactors of 5PTase13. We focused on 5PTase13 because it contains several conserved WD40 repeats (for review, see van Nocker and Ludwig, 2003) and the presence of WD40 repeats within 5PTase genes is unique to plants and certain fungi (Zhong and Ye, 2004). To date, the WD40 repeats of 5PTases have not been functionally characterized, and no potential protein partners have been identified. We show here an important and novel interaction between the WD40 repeat region of 5PTase13 and the central metabolic regulator, SnRK1.1. SnRK1.1 and its orthologues in yeast and mammals is one subunit of a complex that modulates cellular metabolism in response to nutrient and environmental conditions (Baena-Gonzalez et al., 2007; Hardie, 2007; Hue and Rider, 2007). Recent work in Arabidopsis has elegantly delineated the role of SnRK 1.1 in the transcriptional activation of genes from catabolic pathways that provide routes for alternative energy sources and coordinate repression of a large number of anabolic genes (Baena-Gonzalez et al., 2007). Our discovery of a
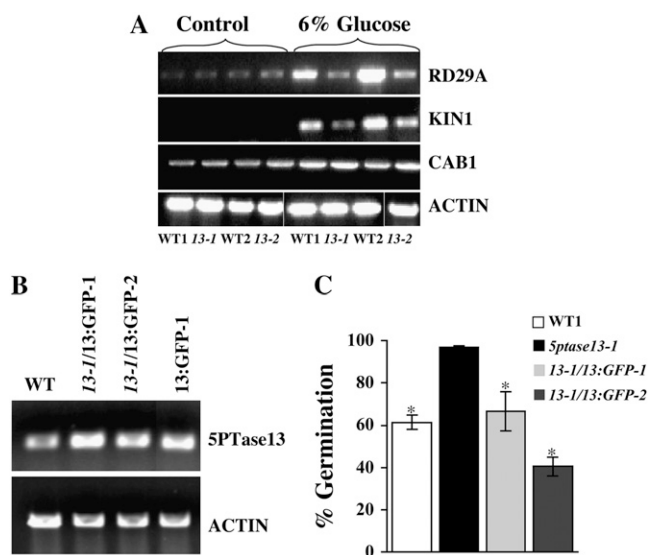
Figure 9. A, Expression of Glc- and ABA-inducible genes from dark-grown 4-d-old wild-type and *5ptase13* seedlings that were either untreated (control; 0.5× MS salts, 0.8% agar) or treated with 6% Glc (0.5× MS salts, 0.8% agar) in the dark for 3 d. The experiment was independently repeated two times. B, Verification of overexpression of 5PTase13 in complemented lines and a 5PTase13:GFP line. Total RNA (1–2 μg) was isolated, and semiquantitative RT-PCR was performed with the indicated primers (Supplemental Table S4). C, The 5PTase13:GFP gene complements the ABA-insensitive phenotype of *5ptase13-1* mutants. Seeds from WT1, *5ptase13-1*, and *5ptase13-1* containing a 5PTase13:GFP transgene were germinated and grown in the light for 6 d on 0.5× MS salts, 0.8% agar, and 3 μM ABA. The germination rate was scored for each group of seeds at day 3. Values are means ± SE ($n = 50$). The experiment was independently repeated two times. *, $P < 0.05$ compared with the *5ptase13-1* mutant.

variability of the root growth phenotype under different nutrient conditions is thus similar, although not identical, to growth responses of SnRK1.1 mutants. In addition, we documented that *5ptase13* mutants are altered in their responses to ABA and sugar stress (Figs. 8–10). When *5ptase13* mutants are challenged with a sugar stress, alterations in germination, gene expression, and InsP$_3$ accumulation occur, indicating that *5ptase13* mutants are sugar insensitive. This sugar insensitivity is similar to that noted for the *regulator of G-protein signaling1* mutant (Chen et al., 2006b) but differs from the Glc-insensitive (Zhou et al., 1998; Arenas-Huertero et al., 2000; Moore et al., 2003; Lin et al., 2007) and sugar-insensitive (Laby et al., 2000; Gibson et al., 2001) mutants that are also insensitive to the developmental arrest induced by sugar that occurs over a period of 21 d. Since there are other WD40-containing 5PTases, we speculate that the sensitivity to developmental arrest noted in *5ptase13* mutants grown on high sugar may be due to this redundancy. Together, the data on nutrient and sugar stress responses of *5ptase13* mutants are consistent with the existence of a 5PTase13:SnRK1.1 complex that modulates seedling responses to nutrient conditions and stress.

To understand how a 5PTase13:SnRK1.1 complex might regulate nutrient and stress signaling, we measured SnRK1 activity in *5ptase13* mutants and wild-type seedlings grown under different nutrient conditions. Our data show that the presence of 5PTase13 affects SnRK1 activity and that nutrient availability is an important switch in 5PTase13 regulation of SnRK1.1. Specifically, 5PTase13 is required to maintain wild-type levels of SnRK1 activity when low nutrient or
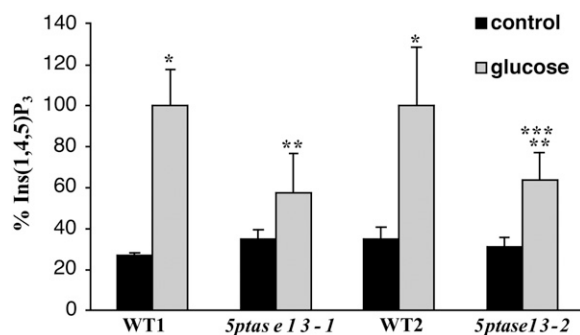
5PTase13:SnRK1.1 complex points to the novel interaction of this metabolic modulator and InsP$_3$ signaling.

It has been shown previously that a loss of function in the 5PTase13 gene leads to defects in auxin-regulated development (Lin et al., 2005) and in blue light responses (Chen et al., 2008). Because of the 5PTase13 interaction with SnRK1.1, we investigated the role of 5PTase13 in nutrient sensing and stress responses. Recent studies have shown that Arabidopsis plants overexpressing SnRK1.1 have greater Suc sensitivity and that mutants lacking SnRK1.1 use exogenous sugars more efficiently (Baena-Gonzalez et al., 2007). When virus-induced gene silencing is used to silence both SnRK1.1 and SnRK1.2, growth is severely affected, indicating the importance of the SnRK1 modulator to overall growth (Baena-Gonzalez et al., 2007). Repressing a pea (*Pisum sativum*) homolog of SnRK1 with antisense RNA results in seed maturation effects resembling ABA insensitivity (Radchuk et al., 2006), while a loss of function in SnRK1 in rice (*Oryza sativa*) delays seed germination and seedling growth (Lu et al., 2007). We report here that *5ptase13* mutants exhibit reduced root growth under limited nutrient conditions, but not when 3% Suc is supplied. The

Figure 10. Comparison of mass InsP$_3$ levels in wild-type and *5ptase13* seedlings. Dark-grown 4-d-old wild-type and *5ptase13* seedlings were untreated (control; 0.5× MS salts, 0.8% agar) or treated with 6% Glc and 0.5× MS salts for 3 d. The seedlings were frozen in liquid nitrogen, ground, and analyzed for mass InsP$_3$ levels as described in "Materials and Methods." Values for InsP$_3$ (pmol g^{-1}) were normalized to the matched wild-type Glc-treated sample; raw values are found in "Materials and Methods." Bars represent means ± SE of three to five replicates. The experiment was repeated three times. *, $P < 0.05$ compared with the control, untreated sample; **, $P < 0.10$ compared with the matched wild-type Glc sample; ***, $P < 0.10$ compared with the control, untreated sample.

Figure 11. Subcellular localization of GFP-tagged 5PTase13 in Arabidopsis seedlings. GFP-tagged 5PTase13 (13:GFP) was expressed in the *5ptase13-1* mutant background, and the subcellular location in cotyledons (A–C) and roots (D–I) from 7-d-old seedlings was examined with fluorescence deconvolution microscopy. A, Differential interference contrast. B, D, and G, GFP fluorescence. C, Overlay of A and B. E and H, Seedlings were stained with DAPI and examined with a standard UV fluorescence filter set. F and I, Overlay of GFP and DAPI fluorescence. Note that red arrows in C indicate nuclei from guard cells expressing 13:GFP, while yellow arrows correspond to nuclei lacking expression. Bars = 20 μm.
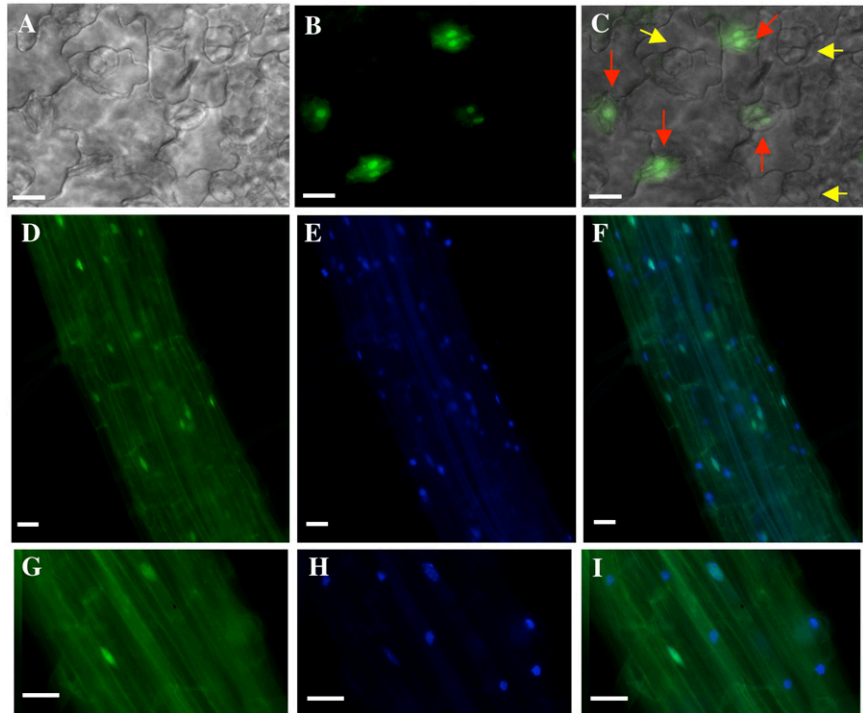
high sugar is present (Fig. 6, B and C). In contrast, under the greatest starvation conditions of no added nutrients, 5PTase13 appears to be a negative regulator of SnRK1, as *5ptase13* mutants contain significantly elevated SnRK1 activity (Fig. 6A). To further delineate the mechanism of 5PTase13 regulation of SnRK1.1, we used a cell-free degradation assay and showed that the decrease in SnRK1 activity in *5ptase13* mutants correlates with increased degradation of SnRK1.1 by the proteasome (Fig. 7D).

Interestingly, another WD40 repeat-containing protein called PRL1 (for PLEITROPIC REGULATOR LOCUS1) also interacts with SnRK1.1 and is able to inhibit the activity of SnRK1.1 and SnRK1.2 (Bhalerao et al., 1999; Farras et al., 2001). Recent evidence shows that there is a decrease in SnRK1 degradation in *prl1* mutant extracts, and additional evidence suggests that PRL1 acts in delivering SnRK1 to the CUL4-DDB1 complex for proteasomal degradation (Lee et al., 2008). Thus, we predict that 5PTase13 and PRL1 have opposing functions regarding SnRK1 stability under low-nutrient and sugar-stress conditions. The fact that *prl1* mutants are ABA and sugar hypersensitive (Bhalerao et al., 1999), which is the opposite of *5ptase13* mutants, also supports opposing roles for 5PTase13 and PRL1 in regulating SnRK1 degradation.

Our data reported here, along with data from other groups, support the model of SnRK1 as a sensor of low nutrient status and cellular stress. Under low-nutrient or sugar-stress conditions, 5PTase13 acts as a positive regulator of SnRK1.1 activity by reducing the amount of SnRK1 targeted for proteasomal destruction. This

regulation most likely involves a 5PTase13-SnRK1.1 interaction within the nucleus, as that is where we find 5PTase13:GFP (Fig. 11), and SnRK1 is most likely nuclear as well (Pierre et al., 2007; Thelander et al., 2007). A loss of 5PTase function, therefore, results in a lack of response, or insensitivity, to stress conditions. In contrast, nuclear PRL1 acts as a negative regulator of SnRK1.1 and facilitates its proteasomal destruction. Thus, the increased SnRK1 levels found in *prl1* mutants could potentiate low-nutrient and/or stress signaling, resulting in the hypersensitivity to sugar and ABA found in this mutant. Nemeth et al. (1998) showed that PRL1 is located in the nucleus, as are CUL4 and other SnRK1-interacting proteasomal components such as SKP/ASK1 and a4/PAD1 (Farras et al., 2001; Chen et al., 2006a).

While data support this model, we currently do not know how second messenger $InsP_3$ affects the SnRK1 pathway. We have shown that $InsP_3$ levels increase when seedlings are given a sugar stress, implicating $InsP_3$ as a second messenger under high-sugar conditions (Fig. 10). Given that the 5PTase13 enzyme has been shown to hydrolyze $InsP_3$ in vitro (Zhong and Ye, 2004), we expected that a loss of 5PTase13 function would elevate $InsP_3$. However, *5ptase13* mutants have, instead, lower $InsP_3$ levels upon sugar stress (Fig. 10). The lack of increase in Glc-stimulated $InsP_3$ accumulation in *5ptase13* mutants may indicate a more complex role for $InsP_3$ in 5PTase13 function and/or could be the result of compensatory actions of the other 5PTase enzymes. Elevated $InsP_3$ levels have been found in other *5ptase* mutants, and this increase in

$InsP_3$ is sometimes associated with ABA hypersensitivity (Carland and Nelson, 2004; Gunesekera et al., 2007). It should be noted that *5ptase13* mutant seeds are also ABA insensitive, a trait they share with other sugar-insensitive mutants. It is currently thought that the sugar-induced delay of germination involves the action of ABA, as ABA synthesis mutants are also resistant to the effects of sugars (Price et al., 2003; Rognoni et al., 2007).

There have been previous reports that inositol signaling and sugar sensing/metabolism are linked. Im et al. (2007) found that expressing a human phosphatidylinositol 4-phosphate 5-kinase (PIP5K) gene in tissue culture cells dramatically elevated phosphatidylinositol 4,5-bisphosphate ($PtdInsP_2$) and $InsP_3$ and resulted in increased sugar use and oxygen uptake. This work importantly defined the PIP5K enzyme as the flux-limiting enzyme for $PtdInsP_2$ production and $InsP_3$ signaling in plant cells. In separate studies, Lou et al. (2007) found that one member of the PIP5K gene family, At3g09920, negatively regulates a cytosolic invertase by direct protein interactions. These investigators found that a gain of function in this same PIP5K gene results in less invertase activity and a resulting sugar insensitivity in transgenic seedlings. Additional evidence supporting the importance of $PtdInsP_2$ in sugar sensing/metabolism comes from transcriptional studies. A rigorous correlative analysis of gene expression shows that a different PIP5K gene (At4g17080) is one of 278 genes coactivated by SnRK1.1 and sugar starvation and down-regulated by sugar treatment (Baena-Gonzalez et al., 2007). Together, these studies indicate that PIP5K-catalyzed production of $PtdInsP_2$ may play a critical role in mediating the response of plant cells to sugar. In addition to transcriptional changes in PIP5K, protoplasts overexpressing SnRK1.1 repress two genes required for inositol synthesis (At4g39800 and At3g02870) and activate three genes encoding other 5PTases (5PTase1, 5PTase12, and FRA3; Baena-Gonzalez et al., 2007). These alterations indicate the likelihood that the SnRK1 modulator decreases the energy-consuming synthesis of inositol but increases the ability of the plant cell to hydrolyze inositol-containing second messengers such as $InsP_3$.

Together, the data presented here support a unique role for 5PTase13 functioning as a binding partner and regulator of the SnRK1.1 modulator of energy and stress signaling. Given the previously established role of 5PTase13 in blue light signaling (Chen et al., 2008), this work identifies a new connection between inositol signaling and the sensing of cellular metabolism, energy, light, and stress.

MATERIALS AND METHODS

Phylogenetic Tree Construction

BLASTp was used to identify 12 related WD40 regions. ClustalW and PAUP4.0 were used to generate phylogenetic trees using parsimony. One thousand bootstraps were performed.

Yeast Two-Hybrid Screen

The Matchmaker Two-Hybrid System 3 was used (BD Biosciences Clontech). The cDNA corresponding to amino acids 1 to 533 of 5PTase13 was amplified by PCR and ligated into pGBKT7 bait vector (BD Biosciences Clontech), verified by DNA sequencing, and transformed into yeast strain AH109. The yeast strain AH109 containing the 5PTase13 WD40 repeat domain was transformed with an Arabidopsis (*Arabidopsis thaliana*) 3-d-old etiolated seedling cDNA library (Thelogis). Screening for interactors was performed with SD/-Ade-His-Leu-Trp, 10 mM 3-amino-1,2,4-triazole, and 20 μg mL^{-1} 5-bromo-4-chloro-3-indolyl-β-D-galactopyranoside plates. Candidate clones that grew were rescued from yeast and retested in the original bait and control strains. Prey plasmids that passed all tests were sequenced to identify the Arabidopsis gene insert.

Mutant Isolation

Arabidopsis ecotype Columbia was used for all experiments. Growth conditions of soil-grown plants have been described (Berdy et al., 2001). Regular-light conditions were 100 μE for 16-h days, while low-light conditions were 40 μE for 16-h days. *5ptase13-1* (At1g05630, SAIL_350_F1) and *5ptase13-2* (SALK_081991) mutants were identified from the SIGnAL database (Alonso et al., 2003). Methods for PCR screening of mutants has been described (Ercetin et al., 2008) and utilized SALK and SAIL LB primers and 5PTase13 gene-specific primers (13-1for, 13-1rev, 13-2for, and 13-2rev; Supplemental Table S4). The resulting PCR fragments were sequenced to map the T-DNA insertions.

Reverse Transcription-PCR

Conditions for reverse transcription (RT)-PCR have been described previously (Ercetin et al., 2008) and used the primers listed in Supplemental Table S4. Amplification of the WD40 region of 5PTase13 was performed using primers 13WD40for and 13WD40rev. Conditions for actin (Berdy et al., 2001), KIN1 (Knight et al., 1998), and RD29A (Sanchez and Chua, 2001) amplification have been described and generate 428-, 342-, and 715-bp products, respectively. Each RT-PCR experiment was independently repeated at least two times to verify the observed changes in expression.

Seedling Growth and Seed Germination Assays

Age-matched seeds used for assays were harvested from plants grown in parallel on the same shelf in a growth room, and seeds were harvested on the same day and ripened for 6 weeks at room temperature. Seeds were surface sterilized and plated on no salts or 0.5× MS salts solution (pH 5.7) containing 0.8% agar. Seeds were stratified on plates at 4°C for 3 d and germinated at 23°C in the light or dark. For seed germination and root growth assays, seeds were plated on medium containing 0%, 1%, 3%, or 6% Glc or mannitol (Sigma-Aldrich) or 0%, 1%, 2%, 3%, 6%, or 11% Suc (Sigma-Aldrich) in the light or dark at 23°C. Germination was scored as positive when the radicle protruded through the seed coat. For ABA sensitivity experiments, ABA (Sigma-Aldrich) was dissolved in 100% ethanol and added to cooled, sterile medium at a final concentration of 1, 2, or 3 μM ABA. The germination assay was performed as before. Hormone/sugar treatment experiments were repeated two or three times.

Immunoprecipitations

The entire open reading frame (encoding 535 amino acids) of At3g01090 was amplified with gene-specific primers SnRK1.1pFor and SnRK1.1pRev (Supplemental Table S4) and ligated to pCRT7/CT-TOPO vector. This resulted in pSnRKV5, which directed expression of a 61.7-kD SnRK1.1 protein with a C-terminal 6xHis tag and V5 epitope tag (Invitrogen). The WD40 repeat region of 5PTase13 was amplified with gene-specific primers WD40For and WD40Rev (Supplemental Table S4) and ligated to pCRT7/NT-TOPO vector. This resulted in p13WDX, which directed expression of a 65.9-kD protein that corresponds to the WD40 region of 5PTase13 and an N-terminal 6xHis tag and Xpress epitope (Invitrogen). For expression, pSnRKV5 and p13WDX were transformed in *Escherichia coli* BL21(DE3) pLysS cells (Invitrogen), and the resulting recombinant proteins 13WDX and SnRKV5 were purified using nickel-nitrilotriacetic acid agarose columns (Invitrogen). SnRKV5 protein

appeared on the SDS protein gel as two separate bands. These bands represented an active SnRKV5 recombinant protein as determined by the SnRK1 activity assay.

For the immunoprecipitation, between 40 and 90 ng of the purified and dialyzed proteins was used. The immunoprecipitation reactions were carried out as described by Ercetin et al. (2008). Western-blot conditions were as described previously (Burnette et al., 2003). For detection of either the V5 or the Xpress epitope tag, a 1:5,000 dilution of the mouse anti-V5 or anti-Xpress monoclonal antibody, followed by a 1:20,000 dilution of goat anti-mouse horseradish peroxidase-conjugated antibody (Amersham), was used. Purified positope protein (175 ng; Invitrogen) was loaded on the same gel to estimate the amount of recombinant V5- or Xpress-tagged proteins.

SnRK1 Activity Assay

Whole 7-d-old seedlings were ground in liquid nitrogen and resuspended in extraction buffer (50 mM Tris-HCl, pH 7.8, 1 mM EGTA, 1 mM EDTA, 2 mM dithiothreitol [DTT], 0.05% Nonidet P-40, 0.5 mM phenylmethylsulfonyl fluoride, 1 mM benzamide, 3 mM glycerophosphate, and plant protease cocktail; Sigma). After centrifugation at 13.2 rpm for 15 min at 4°C, ammonium sulfate was slowly added to the supernatant to 40% saturation while stirring for 10 min at 4°C and centrifuged for 15 min in 13.2 rpm and 4°C. Precipitated protein was resuspended in 50 μL of fractionation buffer (50 mM Tris-HCl, pH 7.8, 1 mM EGTA, 1 mM EDTA, 2 mM DTT, 0.05% Nonidet P-40, 0.5 mM phenylmethylsulfonyl fluoride, 1 mM benzamide, 3 mM glycerophosphate, 10% glycerol, and plant protease cocktail; Sigma). Protein concentration was determined according to the Bradford method (Bradford, 1976), and equal amounts of protein were added to each assay. SnRK1 activity assay was performed as described by Radchuk et al. (2006) with slight modifications. Protein extract (5 μg in 5 μL) was mixed with 5 μL of kinase buffer (50 mM Tris-HCl and 1 mM DTT, pH 7.0), 5 μL of sterile water, 5 μL of SPS peptide stock solution (peptide sequence RDHMPRIRSEMQIWSED; 200 μM), and 5 μL of labeled ATP stock solution (5 mM [γ-^{32}P]ATP, 5 mM unlabeled ATP, and 125 mM magnesium chloride). The samples were incubated for 30 min at 30°C, and 10-μL aliquots were spotted twice onto P81 paper. The pieces were washed three times in 125 mM phosphoric acid for 20 min each and transferred to scintillation vials for counting. Two different control reactions were examined along with each reaction assay. The first reaction control contained no SPS peptide, and the second control contained no protein extract. Activity was expressed as nanomoles of phosphate incorporated into peptide per minute per milligram of protein. The assay was performed using two independently prepared extracts and three replicates of each extract.

Cell-Free Degradation Assay

Conditions described by Lee et al. (2008) were followed. Briefly, 7-d-old light-grown seedlings were ground in liquid nitrogen, resuspended in buffer (25 mM Tris, pH 7.5, 10 mM MgCl$_2$, 5 mM DTT, and 10 mM NaCl), and centrifuged at 13.2 rpm for 10 min at 4°C. Purified recombinant SnRK1.1-V5 (SnRKV5; 500 ng) and total cell extracts (30 μg) were mixed in a reaction buffer (25 mM Tris, pH 7.5, 10 mM MgCl$_2$, 5 mM DTT, 10 mM NaCl, and 10 mM ATP) and incubated at 30°C for the indicated times. Reactions were analyzed by SDS-PAGE, followed by western blotting with a 1:10,000 dilution of goat anti-mouse horseradish peroxidase-conjugated anti-V5 antibody (Amersham). Ponceau S staining was performed to ensure that equivalent amounts of extracts were analyzed.

Mutant Complementation and GFP Imaging

The 3,408-bp coding region of 5PTase13 minus the stop codon was amplified by high-fidelity PCR, confirmed by sequencing, cloned into the pENTR/D-TOPO vector (Invitrogen), and recombined via the Gateway system (Invitrogen) using the manufacturer's instructions into pK7FWG2. The resulting 35S cauliflower mosaic virus promoter:5PTase13:GFP construct was transformed into *Agrobacterium tumefaciens* by cold shock and was used in the transformation of *5ptase13-1* and wild-type plants as described (Bechtold et al., 1993). 13-1/13:GFP seedlings were identified on kanamycin plates and by screening for GFP production using a Zeiss Axioimager microscope equipped with fluorescence optics. Two independent complemented lines with detectable GFP expression (*13-1*/13:GFP-1 and *13-1*/13:GFP-2) were used in growth assays and for subcellular localization. Seven-day-old seedlings were used for imaging utilizing Axiovision software (Zeiss). Z-stack series of 15 to 20 1-μm

sections were collected, and deconvolution with an iterative algorithm was applied. The resulting deconvolved images were reconstituted into a single image using the maximal intensity projection function of Axiovision. To visualize nuclei, seedlings were stained with 1 μg mL^{-1} DAPI (Molecular Probes) solution for 5 min, excess liquid was removed, and the seedlings were mounted in water. Photographs were taken with a Zeiss MC100 camera. GFP was imaged with a filter set consisting of an excitation filter of 540 to 580 nm, a dichroic mirror of 595 nm, and a barrier filter of 600 to 660 nm. DAPI staining was visualized with a standard UV fluorescence filter set.

Extraction and Measurement of Mass InsP$_3$

Filters containing whole 4-d-old dark-grown seedlings were floated on a 6% Glc solution (0.5× MS salts, pH 5.7) or on a control solution (0.5× MS salts, pH 5.7, only) in the dark for 3 d and then frozen in liquid nitrogen at the end of the treatment. Tissues were harvested and mass InsP$_3$ measurements were made as described previously (Gunesekera et al., 2007; Ercetin et al., 2008). The assays were performed in triplicate, and the experiment was repeated two times. Raw values for InsP$_3$ in Glc-treated samples are as follows: WT1, 1,313 ± 203 pmol g^{-1}; WT2, 1,313 ± 372 pmol g^{-1}.

Histological Characterization

The histological analysis was performed as described (Carland et al., 1999) with slight modifications. Seven-day-old wild-type and mutant cotyledons of soil-grown seedlings in a growth room were fixed in ethanol:chloroform:acetic acid solution (6:3:1) overnight at 4°C and cleared sequentially in 80% ethanol, 95% ethanol overnight at 4°C, and 10% NaOH for 1 h at 42°C. Cotyledons then were stained briefly (30 s to 2 min) in 0.002% safranin-O (Sigma). Specimens were mounted on slides in 50% glycerol and visualized with differential interference contrast on a Zeiss Axioimager microscope and Spot digital camera (Zeiss). A total of 50 cotyledons per variant were used.

Supplemental Data

The following materials are available in the online version of this article.

Supplemental Figure S1. GENEVESTIGATOR expression analysis.

Supplemental Figure S2. Validation of the SnRK1 activity assay.

Supplemental Figure S3. *5ptase13* mutants are less sensitive to 6% Glc under light.

Supplemental Figure S4. *5ptase13* mutants are less sensitive to 11% Suc under light.

Supplemental Table S1. Identity of the WD40 regions of 5PTases in Arabidopsis.

Supplemental Table S2. Normal cotyledon vein development patterns in wild-type and *5ptase13* plants.

Supplemental Table S3. Abnormal cotyledon vein development patterns in wild-type and *5ptase13* plants.

Supplemental Table S4. Primer sequences.

LITERATURE CITED

Alonso JM, Stepanova AN, Leisse TJ, Kim CJ, Chen H, Shinn P, Stevenson DK, Zimmerman J, Barajas P, Cheuk R, et al (2003) Genome-wide insertional mutagenesis of Arabidopsis thaliana. Science 301: 653–657

Andersson MX, Kourtchenko O, Dangl JL, Mackey D, Ellerstrom M (2006) Phospholipase-dependent signalling during the AvrRpm1- and AvrRpt2-induced disease resistance responses in Arabidopsis thaliana. Plant J 47: 947–959

Arenas-Huertero F, Arroyo A, Zhou L, Sheen J, Leon P (2000) Analysis of Arabidopsis glucose insensitive mutants, gin5 and gin6, reveals a central role of the plant hormone ABA in the regulation of plant vegetative development by sugar. Genes Dev 14: 2085–2096

Astle MV, Horan KA, Ooms LM, Mitchell CA (2007) The inositol polyphosphate 5-phosphatases: traffic controllers, waistline watchers and tumour suppressors? Biochem Soc Symp 74: 161–181

Baena-Gonzalez E, Rolland F, Thevelein JM, Sheen J (2007) A central integrator of transcription networks in plant stress and energy signalling. Nature 448: 938–942

Bechtold N, Ellis J, Pelletier G (1993) In planta Agrobacterium mediated gene transfer by infiltration of adult Arabidopsis thaliana plants. C R Acad Sci Ser III Sci Vie 316: 1194–1199

Berdy S, Kudla J, Gruissem W, Gillaspy G (2001) Molecular characterization of At5PTase1, an inositol phosphatase capable of terminating IP$_3$ signaling. Plant Physiol 126: 801–810

Berridge MJ (1993) Inositol trisphosphate and calcium signaling. Nature 361: 315–325

Berridge MJ (2007) Inositol trisphosphate and calcium oscillations. Biochem Soc Symp 74: 1–7

Bhalerao RP, Salchert K, Bako L, Okresz L, Szabados L, Muranaka T, Machida Y, Schell J, Koncz C (1999) Regulatory interaction of PRL1 WD protein with Arabidopsis SNF1-like protein kinases. Proc Natl Acad Sci USA 96: 5322–5327

Boss WF, Davis AJ, Im YJ, Galvão RM, Perera IY (2006) Phosphoinositide metabolism: towards an understanding of subcellular signaling. Subcell Biochem 39: 181–205

Bradford MM (1976) A rapid and sensitive method for the quantitation of microgram quantities of protein utilizing the principle of protein-dye binding. Anal Biochem 72: 248–254

Burnette RN, Gunesekera BM, Gillaspy GE (2003) An Arabidopsis inositol 5-phosphatase gain-of-function alters abscisic acid signaling. Plant Physiol 132: 1011–1019

Carland FM, Berg BL, FitzGerald JN, Jinamornphongs S, Nelson T, Keith B (1999) Genetic regulation of vascular tissue patterning in Arabidopsis. Plant Cell 11: 2123–2137

Carland FM, Nelson T (2004) Cotyledon vascular pattern2-mediated inositol (1,4,5) triphosphate signal transduction is essential for closed venation patterns of Arabidopsis foliar organs. Plant Cell 16: 1263–1275

Chen H, Shena Y, Tang X, Yb Y, Wang J, Guoa L, Zhang Y, Zhang H, Feng S, Strickland E, et al (2006a) Arabidopsis CULLIN4 forms an E3 ubiquitin ligase with RBX1 and the CDD complex in mediating light control of development. Plant Cell 18: 1991–2004

Chen X, Lin WH, Wang Y, Luan S, Xue HW (2008) An inositol polyphosphate 5-phosphatase functions in PHOTOTROPIN1 signaling in Arabidopsis by altering cytosolic Ca^{2+}. Plant Cell 20: 353–366

Chen Y, Ji F, Xie H, Liang J, Zhang J (2006b) The regulator of G-protein signaling proteins involved in sugar and abscisic acid signaling in Arabidopsis seed germination. Plant Physiol 140: 302–310

Clement S, Krause U, Desmedt F, Tanti JF, Behrends J, Pesesse X, Sasaki T, Penninger J, Doherty M, Malaisse W, et al (2001) The lipid phosphatase SHIP2 controls insulin sensitivity. Nature 409: 92–97

DeWald DB, Torabinejad J, Jones CA, Shope JC, Cangelosi AR, Thompson JE, Prestwich GD, Hama H (2001) Rapid accumulation of phosphatidylinositol 4,5-bisphosphate and inositol 1,4,5-trisphosphate correlates with calcium mobilization in salt-stressed Arabidopsis. Plant Physiol 126: 759–769

Ercetin M, Ananieva E, Safaee N, Robinson J, Gillaspy G (2008) Phosphoinositide-specific myo-inositol polyphosphate 5-phosphatase required for seedling growth. Plant Mol Biol 67: 375–388

Farras R, Ferrando A, Jasik J, Kleinow T, Okresz L, Tiburcio A, Salchert K, del Pozo C, Schell J, Koncz C (2001) SKP1-SnRK protein kinase interactions mediate proteasomal binding of a plant SCF ubiquitin ligase. EMBO J 20: 2742–2756

Gibson SI, Laby RJ, Kim D (2001) The sugar-insensitive1 (sis1) mutant of Arabidopsis is allelic to ctr1. Biochem Biophys Res Commun 280: 196–203

Gubler F, Millar AA, Jacobsen JV (2005) Dormancy release, ABA and pre-harvest sprouting. Curr Opin Plant Biol 8: 183–187

Gunesekera B, Torabinejad J, Robinson J, Gillaspy GE (2007) Inositol polyphosphate 5-phosphatases 1 and 2 are required for regulating seedling growth. Plant Physiol 143: 1408–1417

Hardie DG (2007) AMP-activated/SNF1 protein kinases: conserved guardians of cellular energy. Nat Rev Mol Cell Biol 8: 774–785

Huang JZ, Huber SC (2001) Phosphorylation of synthetic peptides by a CDPK and plant SNF1-related protein kinase: influence of proline and basic amino acid residues at selected positions. Plant Cell Physiol 42: 1079–1087

Hue L, Rider MH (2007) The AMP-activated protein kinase: more than an energy sensor. Essays Biochem 43: 121–137

Im YJ, Perera IY, Brglez I, Davis AJ, Stevenson-Paulik J, Phillippy BQ, Johannes E, Allen NS, Boss WF (2007) Increasing plasma membrane phosphatidylinositol(4,5)bisphosphate biosynthesis increases phosphoinositide metabolism in Nicotiana tabacum. Plant Cell 19: 1603–1616

Jones MA, Raymond MJ, Smirnoff N (2006) Analysis of the root-hair morphogenesis transcriptome reveals the molecular identity of six genes with roles in root-hair development in Arabidopsis. Plant J 45: 83–100

Kagawa S, Soeda Y, Ishihara H, Oya T, Sasahara M, Yaguchi S, Oshita R, Wada T, Tsuneki H, Sasaoka T (2008) Impact of transgenic overexpression of SH2-containing inositol 5′-phosphatase 2 on glucose metabolism and insulin signaling in mice. Endocrinology 149: 642–650

Knight H, Brandt S, Knight MR (1998) A history of stress alters drought calcium signalling pathways in Arabidopsis. Plant J 16: 681–687

Krinke O, Novotna Z, Valentova O, Martinec J (2007) Inositol trisphosphate receptor in higher plants: is it real? J Exp Bot 58: 361–376

Laby RJ, Kincaid MS, Kim D, Gibson SI (2000) The Arabidopsis sugar-insensitive mutants sis4 and sis5 are defective in abscisic acid synthesis and response. Plant J 23: 587–596

Lee JH, Terzaghi W, Gusmaroli G, Charron JB, Yoon HJ, Chen H, He YJ, Xiong Y, Deng XW (2008) Characterization of Arabidopsis and rice DWD proteins and their roles as substrate receptors for CUL4-RING E3 ubiquitin ligases. Plant Cell 20: 152–167

Lee Y, Kim YW, Jeon BW, Park KY, Suh SJ, Seo J, Kwak JM, Martinoia E, Hwang I (2007) Phosphatidylinositol 4,5-bisphosphate is important for stomatal opening. Plant J 5: 803–816

Li D, Roberts R (2001) WD-repeat proteins: structure characteristics, biological function, and their involvement in human diseases. Cell Mol Life Sci 58: 2085–2097

Lin PC, Hwang SG, Endo A, Okamoto M, Koshiba T, Cheng WH (2007) Ectopic expression of ABSCISIC ACID2/GLUCOSE INSENSITIVE1 in Arabidopsis promotes seed dormancy and stress tolerance. Plant Physiol 143: 745–758

Lin WH, Wang Y, Mueller-Roeber B, Brearley CA, Xu ZH, Xue HW (2005) At5PTase13 modulates cotyledon vein development through regulating auxin homeostasis. Plant Physiol 139: 1677–1691

Lou Y, Gou JY, Xue HW (2007) PIP5K9, an Arabidopsis phosphatidylinositol monophosphate kinase, interacts with a cytosolic invertase to negatively regulate sugar-mediated root growth. Plant Cell 19: 163–181

Lu CA, Lin CC, Lee KW, Chen JL, Huang LF, Ho SL, Liu HJ, Hsing YI, Yu SM (2007) The SnRK1A protein kinase plays a key role in sugar signaling during germination and seedling growth of rice. Plant Cell 19: 2484–2499

Moore B, Zhou L, Rolland F, Hall Q, Cheng WH, Liu YX, Hwang I, Jones T, Sheen J (2003) Role of the Arabidopsis glucose sensor HXK1 in nutrient, light, and hormonal signaling. Science 300: 332–336

Nemeth K, Salchert K, Putnoky P, Bhalerao R, Koncz-Kalman Z, Stankovic-Stangeland B, Bako L, Mathur J, Okresz L, Stabel S, et al (1998) Pleiotropic control of glucose and hormone responses by PRL1, a nuclear WD protein, in Arabidopsis. Genes Dev 12: 3059–3073

Ortega X, Perez LM (2001) Participation of the phosphoinositide metabolism in the hypersensitive response of Citrus limon against Alternaria alternata. Biol Res 34: 43–50

Perera IY, Heilmann I, Chang SC, Boss WF, Kaufman PB (2001) A role for inositol 1,4,5-trisphosphate in gravitropic signaling and the retention of cold-perceived gravistimulation of oat shoot pulvini. Plant Physiol 125: 1499–1507

Perera IY, Hung CY, Brady S, Muday GK, Boss WF (2006) A universal role for inositol 1,4,5-trisphosphate-mediated signaling in plant gravitropism. Plant Physiol **140:** 746–760

Pierre M, Traverso JA, Boisson B, Domenichini S, Bouchez D, Giglione C, Meinnel T (2007) N-Myristoylation regulates the SnRK1 pathway in *Arabidopsis*. Plant Cell **19:** 2804–2821

Price J, Laxmi A, St Martin SK, Jang JC (2004) Global transcription profiling reveals multiple sugar signal transduction mechanisms in *Arabidopsis*. Plant Cell **16:** 2128–2150

Price J, Li TC, Kang SG, Na JK, Jang JC (2003) Mechanisms of glucose signaling during germination of Arabidopsis. Plant Physiol **132:** 1424–1438

Radchuk R, Radchuk V, Weschke W, Borisjuk L, Weber H (2006) Repressing the expression of the SUCROSE NONFERMENTING-1-RELATED PROTEIN KINASE gene in pea embryo causes pleiotropic defects of maturation similar to an abscisic acid-insensitive phenotype. Plant Physiol **140:** 263–278

Rognoni S, Teng S, Arrus L, Smeekens S, Perata P (2007) Sugar effects on early seedling development in Arabidopsis. Plant Growth Regul **52:** 217–228

Sanchez JP, Chua NH (2001) *Arabidopsis* plc1 is required for secondary responses to abscisic acid signals. Plant Cell **13:** 1143–1154

Sasaoka T, Hori H, Wada T, Ishiki M, Haruta T, Ishihara H, Kobayashi M (2001) SH2-containing inositol phosphatase 2 negatively regulates insulin-induced glycogen synthesis in L6 myotubes. Diabetologia **44:** 1258–1267

Sasaoka T, Wada T, Fukui K, Murakami S, Ishihara H, Suzuki R, Tobe K, Kadowaki T, Kobayashi M (2004) SH2-containing inositol phosphatase 2 predominantly regulates Akt2, and not Akt1, phosphorylation at the plasma membrane in response to insulin in 3T3-L1 adipocytes. J Biol Chem **279:** 14835–14843

Takahashi S, Katagiri T, Hirayama T, Yamaguchi-Shinozaki K, Shinozaki K (2001) Hyperosmotic stress induces a rapid and transient increase in inositol 1,4,5-trisphosphate independent of abscisic acid in Arabidopsis cell culture. Plant Cell Physiol **42:** 214–222

Tang RH, Han S, Zheng H, Cook CW, Choi CS, Woerner TE, Jackson RB, Pei ZM (2007) Coupling diurnal cytosolic Ca^{2+} oscillations to the CAS-IP3 pathway in Arabidopsis. Science **315:** 1423–1426

Thelander M, Nilsson A, Olsson T, Johansson M, Girod P-A, Schaefer DG, Zryd J-P, Ronne H (2007) The moss genes PpSKI1 and PpSKI2 encode nuclear SnRK1 interacting proteins with homologues in vascular plants. Plant Mol Biol **64:** 559–573

van Nocker S, Ludwig P (2003) The WD-repeat protein superfamily in Arabidopsis: conservation and divergence in structure and function. BMC Genomics **4:** 50

Wada T, Sasaoka T, Funaki M, Hori H, Murakami S, Ishiki M, Haruta T, Asano T, Ogawa W, Ishihara H, et al (2001) Overexpression of SH2-containing inositol phosphatase 2 results in negative regulation of insulin-induced metabolic actions in 3T3-L1 adipocytes via its 5'-phosphatase catalytic activity. Mol Cell Biol **21:** 1633–1646

Xiong L, Lee B, Ishitani M, Lee H, Zhang C, Zhu JK (2001) FIERY1 encoding an inositol polyphosphate 1-phosphatase is a negative regulator of abscisic acid and stress signaling in Arabidopsis. Genes Dev **15:** 1971–1984

Zhong R, Burk DH, Morrison WH III, Ye ZH (2004) FRAGILE FIBER3, an *Arabidopsis* gene encoding a type II inositol polyphosphate 5-phosphatase, is required for secondary wall synthesis and actin organization in fiber cells. Plant Cell **16:** 3242–3259

Zhong R, Ye ZH (2004) Molecular and biochemical characterization of three WD-repeat-domain-containing inositol polyphosphate 5-phosphatases in Arabidopsis. Plant Cell Physiol **45:** 1720–1728

Zhou L, Jang JC, Jones TL, Sheen J (1998) Glucose and ethylene signal transduction crosstalk revealed by an Arabidopsis glucose-insensitive mutant. Proc Natl Acad Sci USA **95:** 10294–10299

Zimmermann P, Hirsch-Hoffmann M, Hennig L, Gruissem W (2004) GENEVESTIGATOR: Arabidopsis microarray database and analysis toolbox. Plant Physiol **136:** 2621–2632